ELSEVIER

Polymer 41 (2000) 8061–8074

polymer

www.elsevier.nl/locate/polymer

Fracture toughness of nylon 6 blends with maleated ethylene/propylene rubbers

O. Okada[1], H. Keskkula, D.R. Paul*

Department of Chemical Engineering and Texas Materials Institute, Centre for Polymer Research, The University of Texas at Austin, Austin, TX 78712, USA

Received 12 November 1999; received in revised form 16 February 2000; accepted 18 February 2000

Abstract

The fracture of blends of nylon 6 and maleated ethylene–propylene rubber was examined by both the Izod impact test and a single-edge notch three-point bend (SEN3PB) instrumented Dynatup test. The effects of EPR-*g*-MA content, ligament length, method of fracture surface measurement, sample thickness and fracture position in the molded bar on the fracture behavior were investigated. The data were analyzed by plotting the specific fracture energy (U/A) as a function of ligament length. The blends containing a high portion of EPR-*g*-MA in the rubber phase were found to be super tough over the whole range of ligament lengths and under all test conditions. However, a ductile-to-brittle transition was observed with ligament length for marginally tough blends which contained a low content of EPR-*g*-MA in the rubber phase and had a ductile–brittle temperature near or above room temperature; the specimens with short ligament length fractured in a ductile manner, while the specimens with long ligaments showed brittle fracture. The transition ligament lengths were found to be dependent on the rubber particle size. The dual mode of fracture was rationalized by equations for ductile yielding and brittle crack propagation; values of yield stress and critical intensity factor were estimated from these model equations. The dissipative energy density, u_d, was more sensitive to rubber particle size, sample thickness and location in the molded bar than the limiting specific fracture energy, u_o. There is a good correlation between the standard Dynatup impact strength and the parameter u_d for the gate end specimens.

Keywords: Maleated EPR; Nylon 6; Blends

1. Introduction

The fracture behavior of nylon 6/maleated rubber blends has been described recently in some detail [1–13]. Based on these and other reports, it is clear that the rubber phase morphology critically affects mechanical behavior. For a fixed rubber content of about 20 wt.%, super-tough blends are obtained provided the rubber particle size is greater than a lower limit of about 0.1 μm, but smaller than an upper limit of about 1 μm [7–9].

Maleic anhydride grafted ethylene–propylene elastomers, EPR-*g*-MA, are frequently used for toughening polyamides. Commercial products of this type typically contain approximately 1% by weight of grafted maleic anhydride and give rise to a rubber particle population in a nylon 6 matrix that is in a satisfactory size range for toughening. For example, two recent reports describe such blends containing rubber particles with a weight average diameter, $\bar{d}_w$, of about 0.4 μm that are super-tough down to very low temperature [8–10]. However, if the rubber particle size is decreased through the use of EPR-*g*-MA of higher maleic anhydride content or increased by diluting the rubber phase with an unmaleated EPR, significant reductions of blend toughness can be expected at some point based on published observations for blends of nylon 6 with elastomer particles formed from a styrene/hydrogenated butadiene/styrene, SEBS, triblock copolymer [6].

It is the purpose of this paper to examine thoroughly the fracture behavior of blends containing 20% by weight of a rubber phase formed from mixtures of maleated and unmaleated ethylene–propylene rubbers, EPR. It is of particular interest to explore the ductile-to-brittle transition as a function of the rubber particle size resulting from variation of the EPR/EPR-*g*-MA ratio. Various techniques and conditions of impact testing will be used. For instance, impact strength results obtained by instrumented impact testing in a single-edge notch three-point-bend (SEN3PB) configuration will be compared to the standard notched Izod

* Corresponding author. Tel.: +1-512-471-5238; fax: +1-512-471-0542.

E-mail address: drp@che.utexas.edu (D.R. Paul).

[1] Bridgestone Corporation, 1 Kashio-cho, Totsuka-ku, Yokohama 244-8510, Japan.

0032-3861/00/$ - see front matter
PII: S0032-3861(00)00163-4

Table 1
Material used in this study

Polymer	Commercial designation	Characterization[a]	Molecular weight[a]	Barbender torque[b] (N m)	Source
Nylon 6	Capron 8207F	End-group content: $[NH_2] = 47.9$ meq kg^{-1} $[COOH] = 43.0$ meq kg^{-1}	$\bar{M}_n = 22,000$	5.4	AlliedSignal Inc.
EPR-*g*-MA	Exxelor 1803	43 wt.% ethylene 53 wt.% propylene 1.14 wt.% MA	–	8.2	Exxon Chemical Co.
EPR	Vistalon 457	43 wt.% ethylene 53 wt.% propylene	$\bar{M}_n = 54,000$ $\bar{M}_w/\bar{M}_n = 2$	10.3	Exxon Chemical Co.

[a] Ref. [14].
[b] Torque value taken after 10 min at 240°C and 60 rpm.

strengths. Toughness parameters obtained using 1/8-in. (3.18 mm) and 1/4 in. (6.35 mm) thick specimens, with sharp notches and varying ligament lengths, are explored. These techniques provide a sensitive method of analysis of the change from ductile-to-brittle mode of fracture due to compositional and morphological variations.

2. Experimental

Table 1 describes the materials used in this study. The nylon 6 is a commercial product of AlliedSignal designated as Capron 8207F which is a medium molecular weight grade ($\bar{M}_n = 22,000$) having nearly equivalent amounts of acid and amine end groups. Blends of this nylon 6 with a dispersed phase of ethylene/propylene copolymer of varying particle size were formed by controlling the degree of maleation in the rubber phase by adjusting the ratio of EPR to EPR-*g*-MA. Table 2 shows the compositions of the blends studied and their characteristics.

The materials were dried in a vacuum oven for a minimum of 16 h at 80°C prior to any processing steps. The bale form of non-maleated EPR was cut into strips ($2 \times 4 \times 5$ cm^3) and used to form a masterbatch of 50% EPR and 50% nylon 6 by melt blending in a 250 ml Brabender Plasticorder [14]. For the final blend all component were first vigorously mixed in a plastic bag followed by extruding twice at 240°C and 40 rpm in a Killion single screw extruder ($L/D = 30$, $D = 2.54$ cm) outfitted with an intensive mixing head. The blends were injection molded at 240°C into Izod bars (ASTM D256) that were either 3.18 mm or 6.35 mm thick using an Arburg Allrounder injection molding machine. Molded specimens were kept in a dessicator under vacuum to avoid water sorption.

The morphology of the blends was observed by a JEOL 200 CX transmission electron microscope at −50°C, typically in the plane parallel to the injection flow direction at the center of thick (6.35 mm) samples in the region of fracture near the gate end of an Izod bar. The nylon 6 phase was stained by exposure of thin sections to a 2% aqueous solution of phosphotungstic acid for 30 min at room temperature. The TEM was operated at an accelerating voltage of

Table 2
Morphology and impact strength for 80% nylon 6 + 20% rubber blends

Rubber phase composition	Rubber particle		Izod (J/m)	Ductile–brittle transition temperature (°C)	Dynatup (J/m)		
	$\bar{d}_w$(μm)	Polydispersity	3.18 mm Thickness Standard notch		6.35 mm Thickness		
					Standard notch	Sharp notch	
						2 mm Ligament	10 mm Ligament
0% EPR-*g*-MA + 100% EPR	1.50	3.49	153	40	148	16	63
12.5% EPR-*g*-MA + 87.5% EPR	1.39	1.67	142	40	161	51	96
25% EPR-*g*-MA + 75% EPR	1.10	1.95	334	35	181	41	106
37.5% EPR-*g*-MA + 62.5% EPR	0.75	1.61	405	20	275	69	277
50% EPR-*g*-MA + 50% EPR	0.61	1.89	672	−5	592	55	601
75% EPR-*g*-MA + 25% EPR	0.36	1.58	678	−20	660	55	636
100% EPR-*g*-MA + 0% EPR	0.24	1.75	552	−25	574	57	538

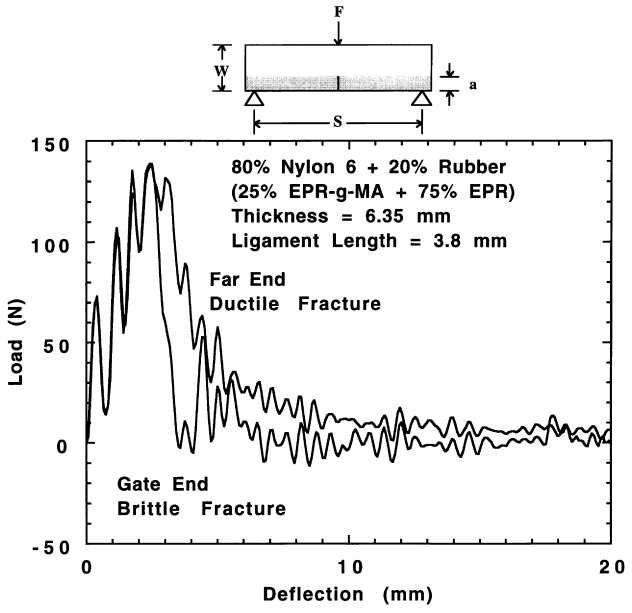

Fig. 1. Load–deflection curves obtained by Dynatup testing of thick specimens with a sharp notch and a ligament length of 3.8 mm for the blends based on a mixture of 25% EPR-*g*-MA and 75% EPR.

120 kV. Rubber particle size was determined by a semi-automated digital analysis technique using IMAGE® software from the National Institutes of Health.

Instrumented impact tests were made using a Dynatup Drop Tower Model 8200 by dropping a 10 kg weight at a speed of 3.5 m/s onto the center of a specimen ($l = 54$ mm) with a span, S, of 48 mm between supports. The specimen geometry was a SEN3PB having an original ligament length ranging typically from 2 to 10 mm with a sharp notch made by a fresh razor blade cooled in liquid nitrogen. The size of the fracture ligaments was determined by two procedures: (a) by measuring the actual length, ℓ_a, of the fractured ligament (from the original crack tip to the beginning of the hinge), from which the actual fracture area can be calculated and (b) by measuring the potential length, ℓ, of the ligament (from the original crack tip to the edge of the test specimen) from which the potential fracture area can be calculated. Most of the specific fracture energies reported here are based on the potential fracture area calculated by the product of specimen thickness and potential ligament length, i.e. method (b). In the case of ductile fractures, procedure (a) gives a shorter ligament length (i.e. hinge type failure), so the fracture energy per unit area is higher. Use of procedure (b) gives a more conservative value of the specific fracture energy. The fracture energy was calculated from the load–deflection curve. Two typical load–deflection curves to be discussed later are shown in Fig. 1 They were signal-conditioned using a digital low pass filter to reduce noise vibration for both ductile and brittle fracture. Correction for drift in the baseline was made on all measurements. Energy losses caused by friction and contact of the specimen and the instrument were eliminated to determine the energy consumed due to fracture. Details of the testing procedure are described elsewhere [9,15].

3. Treatment of fracture data with varying ligament size

Impact fracture energies were measured using both Dynatup and Izod instruments employing molded test specimens of practical dimensions, i.e. 3–6 mm in thickness, t, with sharp notches. The effect of the ligament length on the fracture energy has been analyzed by two mathematically similar methods. Both of these methods are based on the ideas introduced by Broberg [16]. He suggested that the region around the crack consists of an elastic zone where the fracture initiation occurs and a plastic zone where the energy is absorbed during crack propagation. Mai and coworkers [17–19] proposed partitioning the total work of fracture W_f or U into two parts, i.e.

$$W_f = W_e + W_p \tag{1}$$

where W_e is the "essential" work of fracture while W_p is called the "non-essential" work. The first term represents the energy required to create two new surfaces, while W_p is a volume energy term and is proportional to ℓ^2 (ℓ = ligament length). Accordingly, the total fracture work may be rewritten as the specific total fracture work w_f

$$w_f = \left(\frac{W_f}{t\ell}\right) = w_e + \beta w_p \ell \tag{2}$$

where β is a plastic zone shape factor. In this analysis w_p is not a material parameter, but is dependent on specimen geometry. Vu-Khanh [20] proposed an analogous relationship

$$\frac{U}{A} = G_i + \frac{1}{2} T_a A \tag{3}$$

where A is the area of the ligament to be broken, $A = \ell t$. The term G_i has been called the fracture energy at crack initiation and T_a has been identified as a tearing modulus. The interpretation of the slope and intercept terms of plots of U/A vs A is subject to some debate [19]; however, the intercept term does appear to be similar in value to the critical J-integral for fracture, J_{IC} [20].

Test conditions used in this work are similar to those used by Vu-Khanh (thick specimens in bending under high speed loading); however, the results will be analyzed utilizing a mathematical convention similar to the "essential work of fracture" (EWF) method used by Mai et al.. Since we are using different testing conditions and sample geometries than generally used in the EWF methodology, it is not yet clear that the parameters will have exactly the meaning associated with Eq. (2). Thus, for now we adopt a different nomenclature for the intercept and slope of plots of w_f vs ℓ, i.e.

$$\frac{U}{A} = u_o + u_d \ell \tag{4}$$

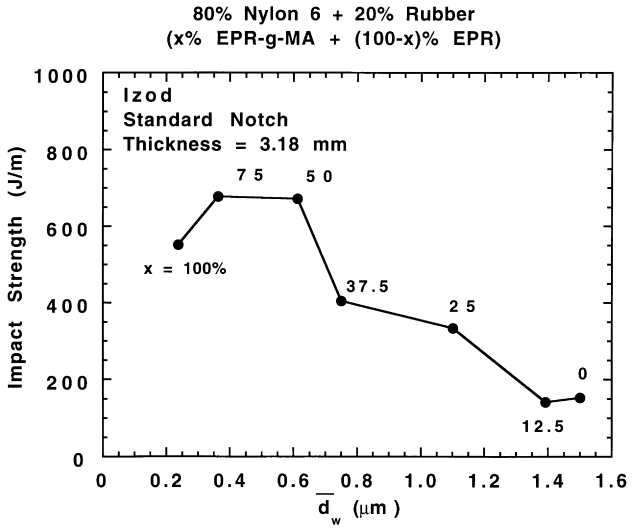

Fig. 2. Izod impact strength as a function of average rubber particle diameter for blends of 80% nylon 6 and 20% maleated EPR mixture.

where U/A is the total fracture energy per unit area, u_o is called the limiting specific fracture energy and u_d is the dissipative energy density in the plastic, stress whitened, zone surrounding the fracture surface [21,22]. In ideal cases, $u_o = w_e$ and $u_d = \beta w_p$.

4. Results and discussion

The characteristics of the blends investigated in this report are summarized in Table 2. As the amount of EPR-*g*-MA in the rubber phase was reduced from 100 to 0% at 20% total rubber, the weight average rubber particle size, $\bar{d}_w$, increased from 0.24 to 1.50 μm. The particle size polydispersity, or the $\bar{d}_w/\bar{d}_n$ ratio, was found to be essentially constant for all blends that contained EPR-*g*-MA in the rubber phase; however, the blend without any reactive rubber component, i.e. 100% EPR, had a significantly higher polydispersity.

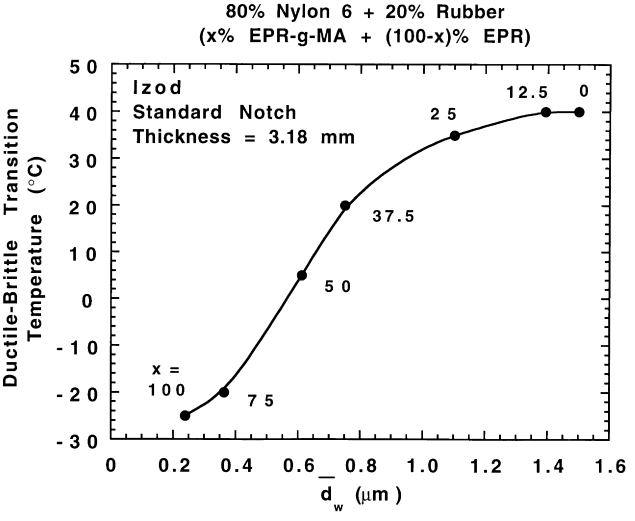

Fig. 3. Ductile–brittle transition temperature as a function of average rubber particle diameter for blends of 80% nylon 6 and 20% maleated EPR mixture.

Standard notched Izod impact strength was determined for the seven EPR-*g*-MA/EPR blends studied. The notched Izod impact strength at room temperature is plotted in Fig. 2 as a function of rubber particle size, $\bar{d}_w$. Super-tough behavior was observed for blends containing 50% or more of the maleated rubber component when the rubber particle diameter is below 0.61 μm. Blends of intermediate toughness were obtained for rubber particles up to 1.1 μm in size. For larger rubber particles, the blends were brittle.

As shown in Fig. 3, the ductile-to-brittle transition temperature is lower the higher the content of EPR-*g*-MA or the smaller the rubber particles. Blends containing less than 37.5% of the maleated rubber, corresponding to rubber particle diameters above 0.75 μm, are relatively brittle at room temperature since the ductile-to-brittle transition temperature is near or higher than room temperature.

Table 2 also shows impact fracture data for 6.35-mm thick specimens with both standard and sharp notches determined in a three-point-bending mode using the Dynatup Drop Tower. The impact fracture energies of specimens with standard notches were substantially the same as determined by the notched Izod test, cantilever mode of fracture, for blends containing 50% or more of EPR-*g*-MA ($\bar{d}_w \leqq 0.61$ μm). However, the largest differences in results from the Izod and Dynatup was seen for compositions with intermediate particle sizes, while at the largest two particle sizes, both methods of testing gave low impact strengths of about 150 J/m.

Impact strengths for thick specimens containing sharp notches and at two ligament lengths (2 and 10 mm) measured by the Dynatup are also shown in Table 2. There was little difference between impact strength of standard notch and sharp notch specimens with 10-mm ligament length for the blends containing 37.5% or more of EPR-*g*-MA in the rubber phase. However, the impact strength for specimens with sharp notches was smaller than for those with standard notches when comparing the blends containing 25% or less of EPR-*g*-MA.

The specimens with a sharp notch and short ligament lengths (2 mm) showed interesting behavior in the Dynatup test. The blend containing 0% EPR-*g*-MA in the rubber phase fractured in a brittle manner at low energy levels (16 J/m), while blends containing from 12.5 to 100% of EPR-*g*-MA fractured in a ductile manner at energy levels of 41 to 69 J/m. These blends were brittle or marginally tough at a ligament length of 10 mm, while the same blends were unexpectedly ductile at a ligament length of 2 mm. These results suggest that a ductile-to-brittle transition result from the change of ligament length for these blends.

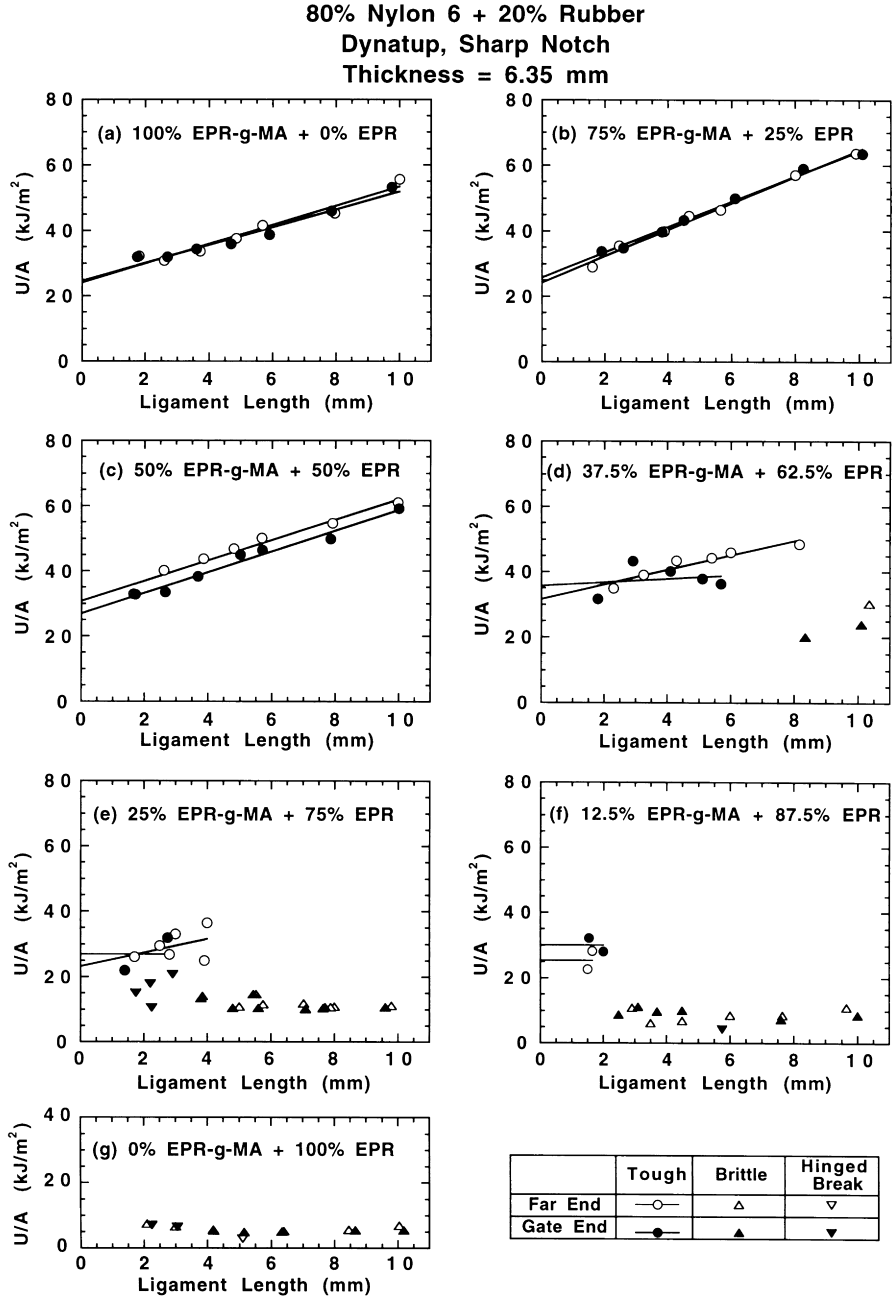

Fig. 4. Fracture energy as a function of ligament length from Dynatup measurements for blends of 80% nylon 6 and 20% rubber using x% EPR-g-MA and $(100 - x)$% EPR for thick specimens with a sharp notch.

4.1. Fracture behavior of single-edge notch three-point-bend specimens

The fracture energy measured as a function of ligament length for 6.35 mm thick specimens in a single notch, three-point-bend mode (like that illustrated at the top of Fig. 1) forms a good linear relationship when plotted as suggested by Eq. (4): the intercept and slope of such plots give the specific limiting fracture energy, u_o, and the dissipative energy density, u_d. Fig. 4 shows typical plots of U/A vs ℓ for 80% nylon 6/20% rubber blends with various ratios of EPR-g-MA to EPR. In addition, the possible effect of the position of the point of fracture along the test bar, relative to the injection gate, was considered. It has been pointed out by Flexman [23–25] that toughened engineering polymers can show significant differences in fracture behavior along the length of an injection-molded bar. He has shown that differences in toughness between the gate and far ends of the bar are greatest in notched Izod tests for blend compositions that fall within a ductile-to-brittle transition region.

As shown in Fig. 4, there is a dramatic change in the relationship between specific fracture energy and ligament

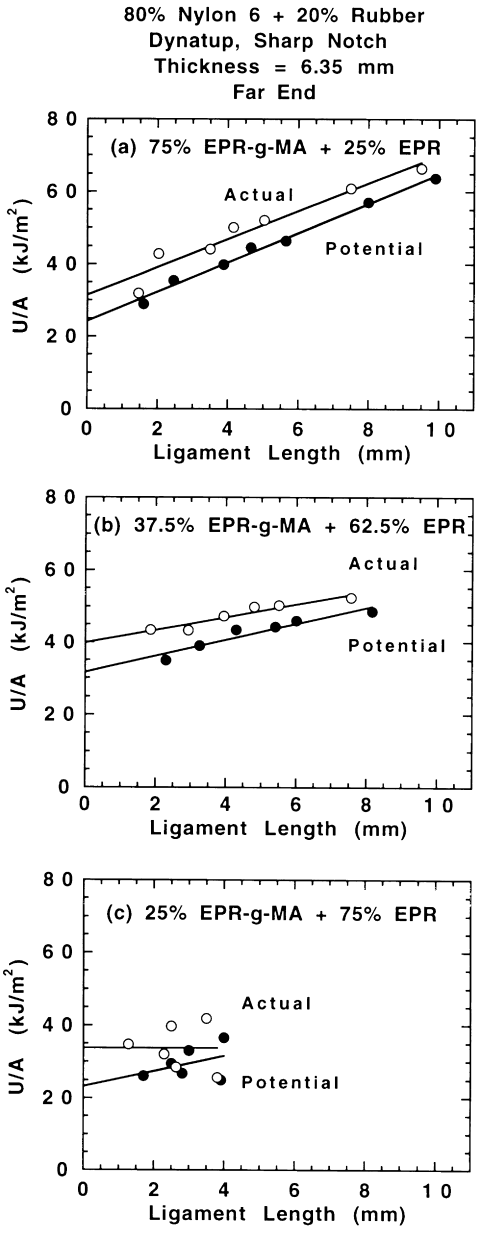

Fig. 5. Fracture energy as a function of potential and actual ligament from Dynatup measurements for blends based on (a) 75% EPR-*g*-MA, (b) 37.5% EPR-*g*-MA and (c) 25% EPR-*g*-MA in the rubber phase.

size as the composition of the rubber phase is altered. In blends containing high levels of EPR-*g*-MA, plots of *U*/*A* vs ℓ are linear with little scatter of the data. For blends that contain 37.5 to 12.5% of the maleated rubber, a single straight line does not describe the results; the specific fracture energy at short ligament lengths is high (failure is ductile) while longer ligaments give much lower values (brittle failure). Obviously Eq. (4) does not describe the data over the full range of ligament length in these cases, at least with a single set of parameters. For comparison purposes, values of u_o and u_d for both ductile and brittle fracture can be computed for specimens that show both types of failure.

As described earlier, method (a) excludes the hinge portion and uses only the ligament that is fractured; naturally this gives higher values of *U*/*A* than when the ligament length is obtained by method (b). Fig. 5 compares *U*/*A* vs ℓ plots obtained from methods (a) and (b) for three selected compositions. The ligament areas represented in Fig. 4 are based on the potential ligament length, i.e. method (b). The fracture parameters obtained by the two methods are listed in Table 3. While the numerical values of these parameters depend on whether ℓ or ℓ_a is used, the trends are similar.

Tables 4 and 5 show the numerical values of the intercepts and slopes, i.e. u_o and u_d obtained from the plots like those in Fig. 4. They reveal that the blends containing 50% or more EPR-*g*-MA are uniformly ductile and have u_o values in the range of 24–31 kJ/m^2 while the u_d values range from 2.7–4.0 MJ/m^3. For the ductile blends, both the gate and far end specimens are uniformly tough at all ligament lengths tested; however, the blends containing 37.5% EPR-*g*-MA or less show a more complicated fracture behavior. It is apparent that as the proportion of unmaleated rubber increases the blends become more brittle. The greatest deviation from the behavior typical of the most ductile blends is seen for EPR-*g*-MA/EPR ratios of 25/75 and 12.5/87.5. Here, the test specimens with the largest ligaments show low values of total specific fracture energy, i.e. *U*/*A*, typical of brittle materials, while those with the smallest ligaments show higher levels. Plots of specific fracture energy vs ligament size with negative slopes have been

Table 3
Fracture Parameters from potential and actual ligament length for Dynatup measurement of far end specimens for nylon 6/rubber (80/20) blends based on mixture of *x*% EPR-*g*-MA and (100 − *x*)% EPR

% EPR-*g*-MA	u_o(kJ/m^2)		u_d(MJ/m^3)	
	Potential ligament	Actual ligament	Potential ligament	Actual ligament
12.5	25.5	28.6	0	0
25	23.3	33.7	2.1	0
37.5	31.7	39.8	2.2	1.8
50	30.8	34.0	3.1	3.3
75	24.2	31.4	4.1	3.9
100	24.1	27.1	3.1	2.9

Table 4
The limiting specific fracture energy, u_o, for nylon 6/EPR (80/20) blends based on varying EPR-*g*-MA content in the rubber phase

	u_o(kJ/m^2)											
	Far end						Gate end					
	Dynatup		Izod				Dynatup		Izod			
	6.35 mm		6.35 mm		3.18 mm		6.35 mm		6.35 mm		3.18 mm	
% EPR-*g*-MA	Ductile	Brittle	Ductile	Brittle	Ductile	Brittle	Ductile	Brittle	Ductile	Brittle	Ductile	Brittle
0	–	6.2	–	8.2	23.8	10.0	–	5.3	–	8.0	20.5	10.5
12.5	25.5	8.6	22.1	9.2	18.4	11.5	30.1	9.2	20.8	8.4	21.5	10.1
25	23.3	11.6	12.5	12.9	17.8	20.1	27.0	11.6	23.3	12.1	23.0	11.3
37.5	31.7	30.2	17.5	–	16.5	–	35.8	21.9	19.7	–	21.5	13.7
50	30.8	–	21.8	–	13.2	–	26.9	–	20.9	–	17.8	–
75	24.2	–	12.9	–	12.7	–	25.8	–	13.5	–	15.4	–
100	24.1	–	16.1	–	10.1	–	24.7	–	13.9	–	12.7	–

reported for high impact polystyrene [26], toughened nylon 6,6 [26] and nylon 6/ABS blends [27]. However, the present results are more dramatic in that they represent a transition from ductile to brittle fracture as might occur in a transition from plane stress to plane strain conditions. Indeed, Wu and Mai [28] have reported such a transition with ligament length; however, they found ductile (plane stress) behavior at large ligament lengths and brittle (plane strain) behavior at small ligament lengths; the opposite of what is observed here.

To further explore the change in mechanism of deformation with ligament size, fracture surfaces of several marginally tough compositions were examined by scanning electron microscopy. Different specimens of the blend based on 25% EPR-*g*-MA in the rubber phase gave either relatively low (brittle, ▲) or high (tough, ○) impact energies at a ligament length of about 3.8 mm as seen in Fig. 4e. It is apparent from the scanning electron photomicrographs of fracture surfaces in Fig. 6 that a sample which shows brittle behavior experiences no matrix yielding at a distance of 2.5 mm from the crack initiation while the sample exhibiting ductile fracture shows extensive yielding and matrix deformation. Fig. 1 compares load-deflection curves for specimens of this composition that show ductile and brittle behavior. The load-deflection traces are identical up to the maximum load of about 140 N; after this, the more ductile specimen shows higher deflection by about 1 mm, apparently due to higher resistance to crack propagation. Its load-deflection trace remains noticeably above that of the brittle specimen indicating a higher total fracture energy. Accordingly, the delayed crack initiation and a crack propagation mode modified by the extensive matrix deformation and yielding (Fig. 6b) account for the higher fracture energy.

4.2. Fracture energy by Notched Izod test

The Izod test (cantilever configuration) was also used to

Table 5
The dissipative energy density, u_d, for nylon 6/EPR (80/20) blends based on varying EPR-*g*-MA content in the rubber phase

	u_d(MJ/m^3)											
	Far end						Gate end					
	Dynatup		Izod				Dynatup		Izod			
	6.35 mm		6.35 mm		3.18 mm		6.35 mm		6.35 mm		3.18 mm	
% EPR-*g*-MA	Ductile	Brittle	Ductile	Brittle	Ductile	Brittle	Ductile	Brittle	Ductile	Brittle	Ductile	Brittle
0	–	0.0	–	0.0	0.0	0.0	–	0.0	–	0.0	0.0	0.0
12.5	0.0	0.0	0.0	0.0	1.7	0.0	0.0	0.0	0.0	0.0	0.0	0.0
25	2.1	0.0	3.2	0.0	3.3	0.0	0.0	0.0	0.0	0.0	0.0	0.0
37.5	2.2	0.0	3.5	–	4.5	–	0.5	0.0	2.3	–	1.4	0.0
50	3.1	–	5.0	–	5.7	–	3.2	–	4.8	–	3.3	–
75	4.0	–	6.0	–	6.4	–	3.9	–	5.7	–	4.6	–
100	2.9	–	2.3	–	6.6	–	2.7	–	2.6	–	5.4	–

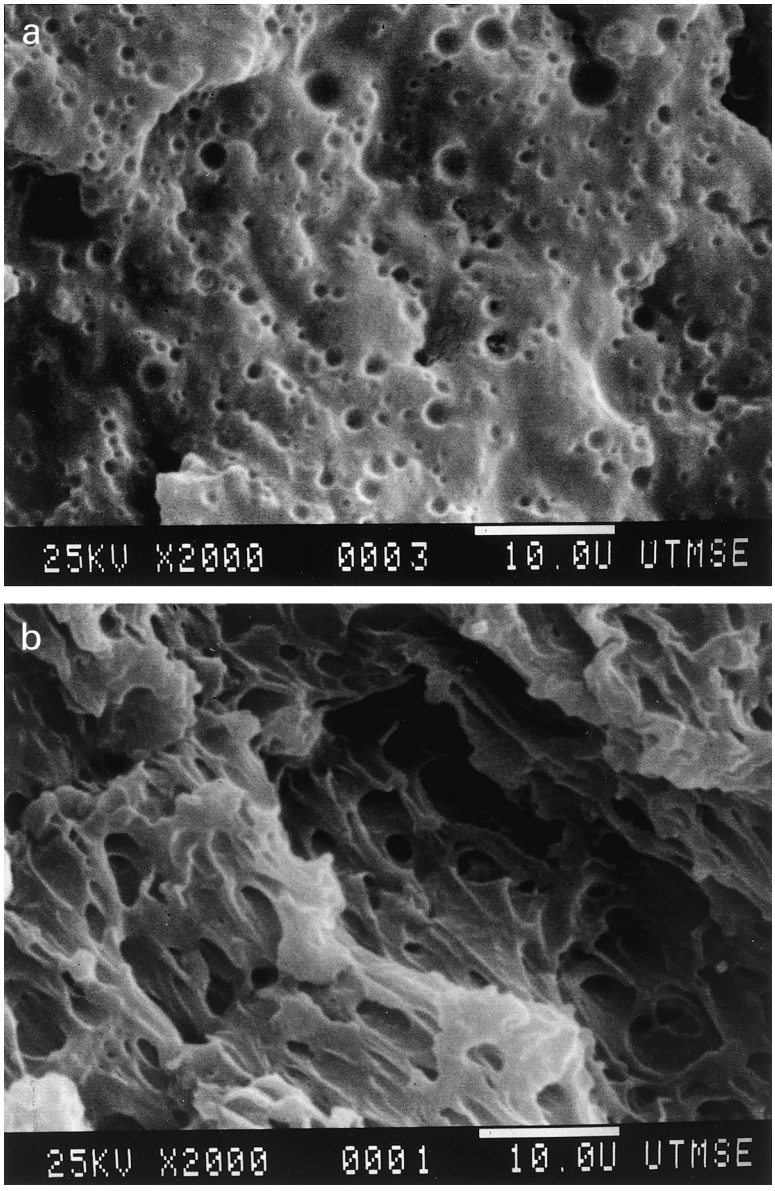

Fig. 6. SEM photomicrographs showing the fracture surface of (a) brittle and (b) ductile fracture for thick specimens with a 3.8 mm ligament length for blends based on 25% EPR-*g*-MA and 75% EPR mixture.

determine the fracture energy as a function of ligament length for specimens with sharp notches for comparison with the fracture behavior in the single-edge notch three-point-bend configuration using the Dynatup. The impact fracture energies for the two tests are compared in Table 2; there is good agreement with similar results reported previously [6–8,10].

Standard notched Izod data are presented in Fig. 2 (as a function of rubber particle size) and in Fig. 3 to show the effect of particle size on the ductile–brittle transition temperature. Fig. 7 shows how the mode of impact fracture (ductile or brittle) of specimens with sharp notches depends on ligament length, sample thickness, and blend morphology. In these diagrams, specimens that exhibited complete break with relatively low specific fracture energy are classified as brittle, while those that exhibited a partial break with high specific fracture energy were considered to have experienced ductile failure. As seen in Fig. 7, rather similar ductile-to-brittle boundaries are obtained from Dynatup and Izod (3.18 or 6.35 mm) testing. No complete, or brittle, breaks were observed when the ligament lengths were of the order of 2 mm or less, even for the more brittle compositions containing 12.5% and 25% EPR-*g*-MA in the rubber phase. Table 6 shows the transition ligament length for the Dynatup test at which the ductile-to-brittle transition occurred. The value of the transition ligament length

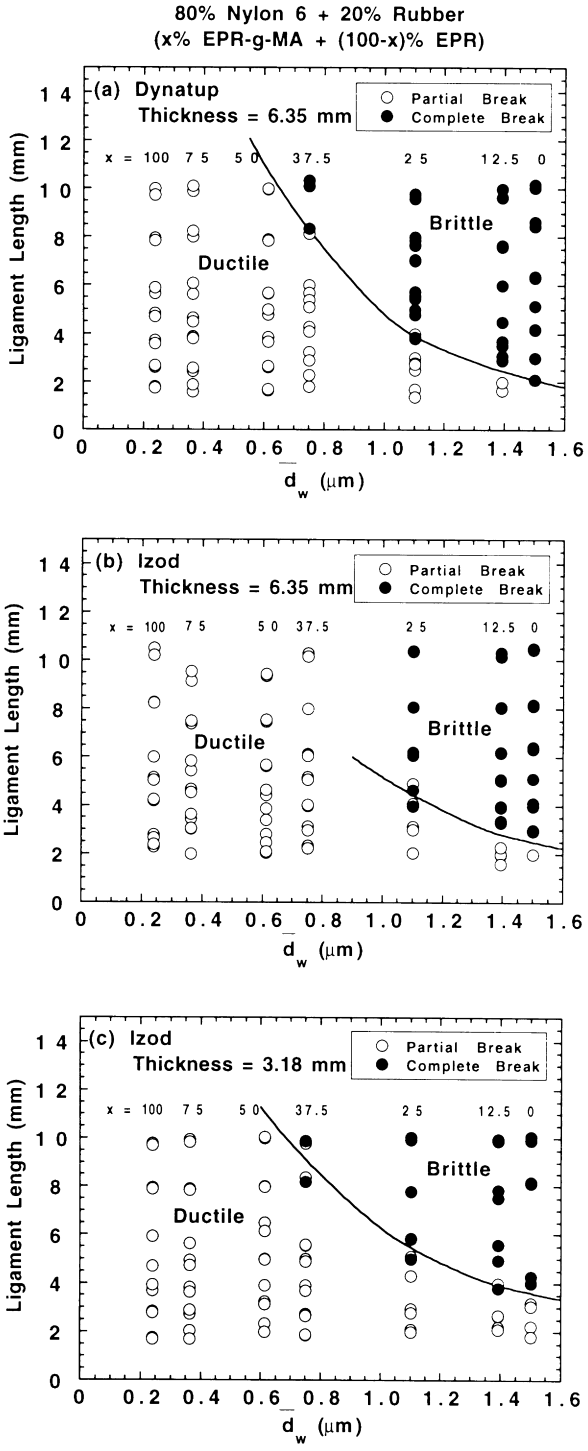

Fig. 7. Failure mode as a function of ligament length and average rubber particle diameter for blends of 80% nylon 6 and 20% maleated EPR mixture measured by: (a) Dynatup for thick specimens, (b) Izod for thick specimens and (c) Izod for thin specimens. Note that all the specimens had sharp notches.

increased with increasing amount of EPR-*g*-MA in the blend, i.e. with decreasing rubber particle size. Kudva et al. [22] have qualitatively explained the transition from ductile to brittle failure as ligament length increases for transitional materials; the basis for this argument will be expanded on later.

Table 6
Fracture parameters from Dynatup for nylon 6/rubber (80/20) blends based on varying EPR-*g*-MA content in the rubber phase

% EPR-*g*-MA	σ_y (MPa)	K_{IC}, Plane-strain stress intensity factor (MPa $m^{1/2}$)	Transition ligament length (mm)
0	–	2.7	2.2
12.5	–	3.2	2.3
25	–	3.5	3.8
37.5	109.3	5.3	7.5
50	101.0	–	–
75	100.3	–	–
100	96.5	–	–

4.3. Comparison of fracture energy parameters

The Izod fracture data for specimens of two thickness (both with sharp notches) are shown in the form of *U*/*A* vs ℓ plots in Fig. 8. The fracture energy parameters u_o and u_d obtained from the Izod and Dynatup (Fig. 4) experiments using various test conditions and specimens are summarized in Tables 4 and 5. The parameters obtained from observed ductile failures for the gate end specimens are plotted in Figs. 9 and 10 as a function of the average rubber particle size. In general, values obtained from Izod and Dynatup testing show similar trends. The parameter u_o seems to generally increase with rubber particle size while u_d goes through a maximum and then decreases. The values of u_o from Dynatup testing are larger than those from the Izod test (Fig. 9a); whereas, the opposite is true for u_d (Fig. 9b). For a given test configuration, u_o is effectively independent of sample thickness while u_d surprisingly appears to be slightly larger for thicker samples. The differences in u_o between specimens from the gate and far ends of injection molded bars are relatively insignificant for all specimens (Fig. 10a); however, for large rubber particles the values of u_d are substantially greater for specimens from the far end of the bar (Fig. 10b). For gate end specimens, there is a good correlation between Dynatup impact strength for the standard notched specimens and u_d (see Fig. 11); however, for far end specimens, the relation is not so direct. Compositions that contain 50% or more of EPR-*g*-MA are uniformly tough in all situations; i.e. when the weight average rubber particle size is 0.61 μm or less. Blends that contain less EPR-*g*-MA (i.e. have larger rubber particles and are marginally tough) are more sensitive to sample dimensions, location in the bar, and test configuration.

4.4. Stress analysis

As mentioned earlier, Kudva et al. [22] have qualitatively

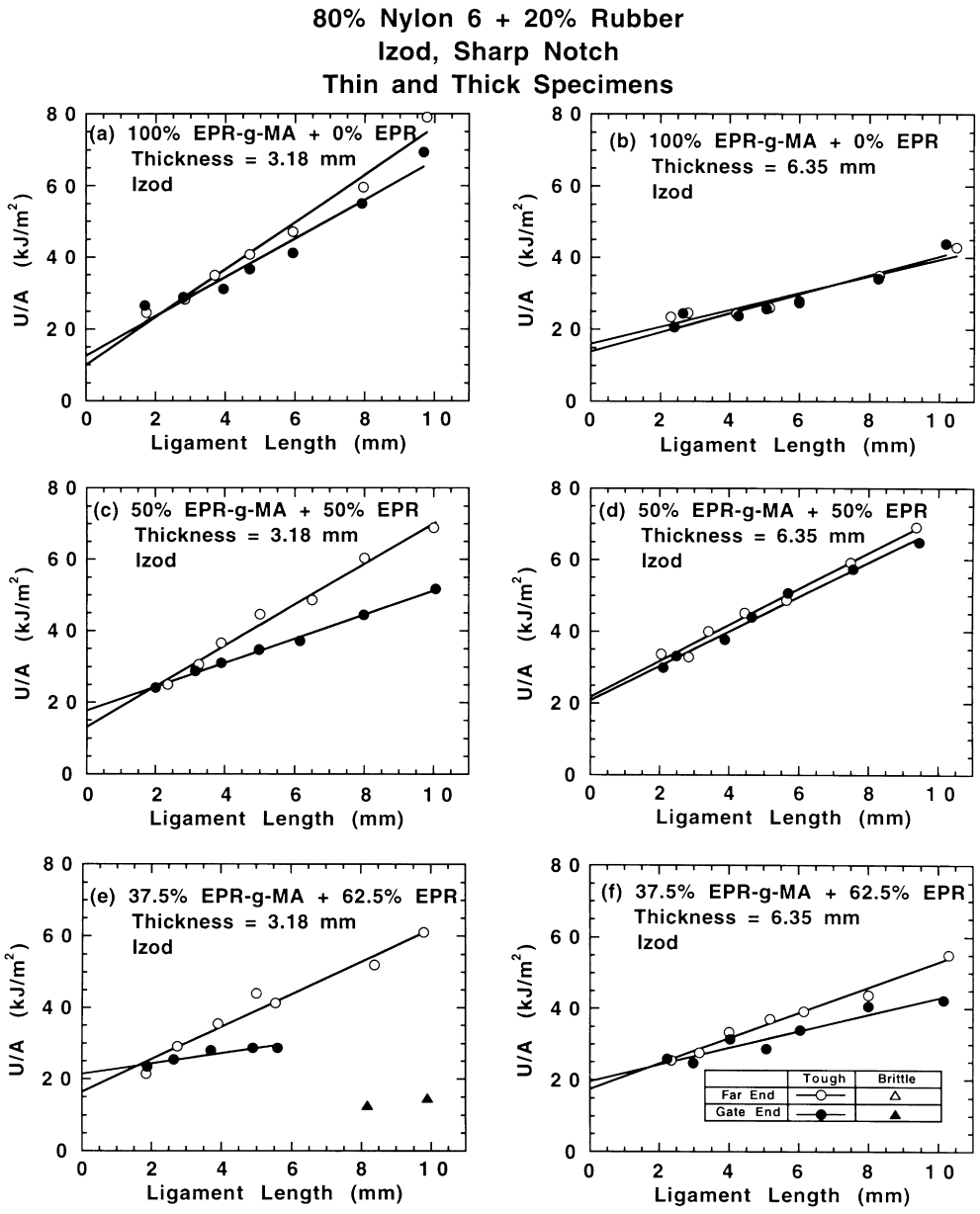

Fig. 8. Fracture energy as a function of ligament length for Izod measurements on thin and thick specimens with a sharp notch for 80% nylon 6 and 20% maleated EPR mixture.

explained the change from ductile to brittle failure as the ligament length increases in terms of the intersection of classical equations describing failure by ductile yielding and brittle crack propagation. McCrum et al. [29] outline the basic argument in terms of simple tension for a specimen with variable crack length; Kudva et al. argued similarly using the analogous equations for bending. The purpose here is to extend this type of analysis using quantitative information from experimental Dynatup force-displacement plots like those in Fig. 1 for a bar loaded in three-point bending (see diagram at top of Fig. 1). The region just below the load goes from a maximum compressive stress at the top of the bar to a maximum tensile stress at the bottom. For a bar without a crack, the maximum tensile stress (at the bottom of the bar) is

$$\sigma_{\max} = \frac{3SF}{2tW^2} \tag{5}$$

according to linear elastic theory [29], where S is the span, t is thickness and W is width. Substitution of the peak load, F, from Dynatup plots (see Fig. 1) into this relation gives a quantity that we will call the failure stress. The results of such calculations are shown in Fig. 12 as a function of the normalized crack length a/W for the various blends. The

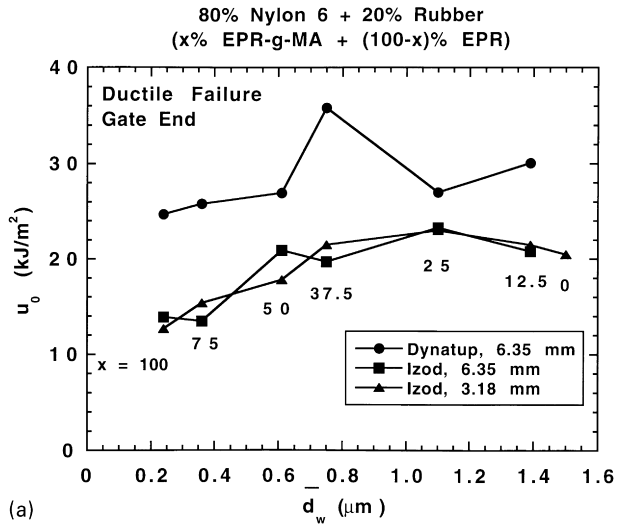

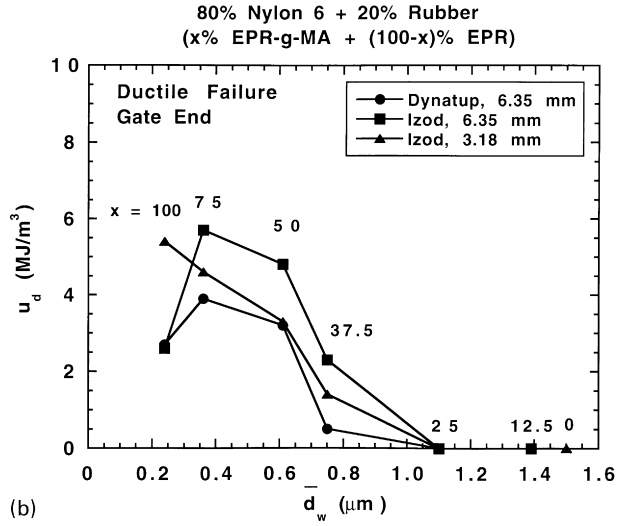

Fig. 9. Fracture parameters for nylon6/maleated EPR blends (20% rubber) (a) u_o vs rubber particle seize (b) u_d vs rubber particle size; specimens were obtained from the gate end of the moldings.

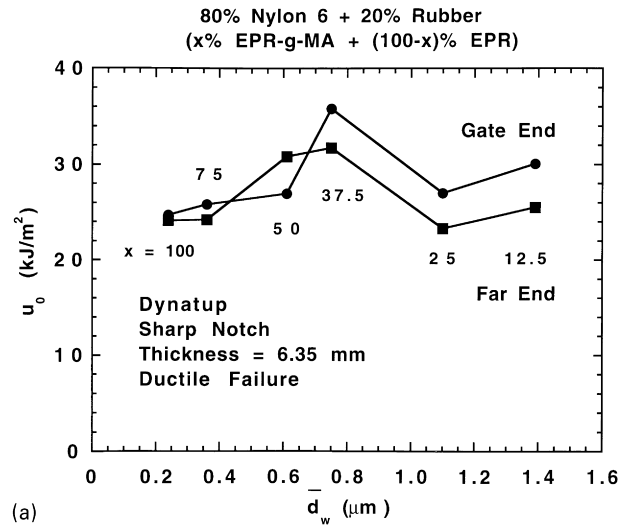

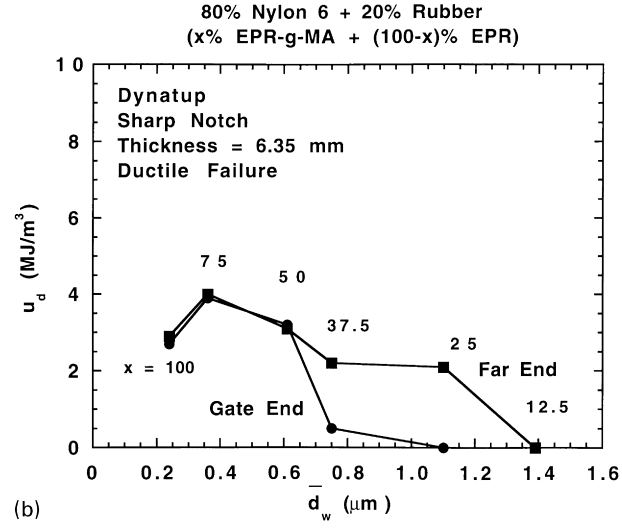

Fig. 10. Comparison of fracture parameters obtained from gate and far ends of 6.35 mm injection molded bars.

open circles represent failures judged to be ductile while the closed circles denote failures judged to be brittle.

Of course, the presence of a crack of length, a, in the bar leads to a more complicated stress pattern and can alter the mode of failure. By the so-called "net section" argument, the tensile stress at the position of the crack tip is given by

$$\sigma_{\max}(a) = \sigma_{\max}(0)\left[\frac{W-a}{W}\right]^2 \tag{6}$$

where $\sigma_{\max}(0)$ is the stress from Eq. (5) where there is no crack, i.e. $a = 0$. The stress given by Eq. (6) amounts to the linear elastic result (Eq. 5) for a bar of width $(W - a)$, i.e. the maximum tensile stress if the shaded material at the top of Fig. 1 were ignored. Thus, if ductile failure occurs by tensile yielding at a stress of σ_y, then the calculated failure stress from Eq. (5) should be [30]

$$\text{failure stress} = \sigma_y\left(\frac{W-a}{W}\right)^2. \tag{7}$$

On the other hand, linear elastic fracture mechanics predicts that under plane-strain conditions brittle failure should occur at [31]

$$\text{failure stress} = \frac{K_{IC}}{Y\sqrt{a}} \tag{8}$$

where K_{IC} is the critical stress intensity factor and Y is a

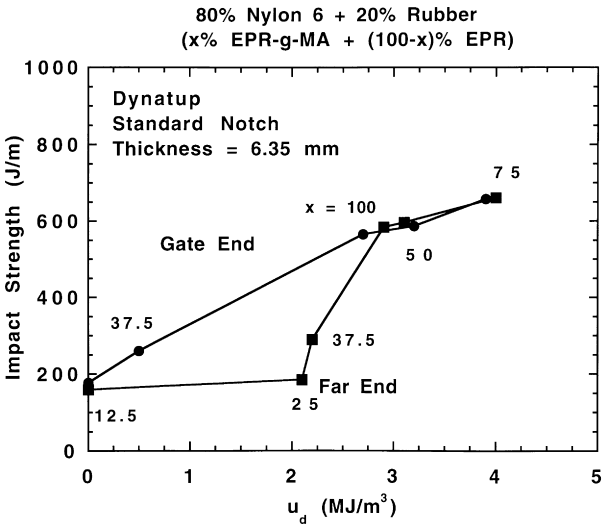

Fig. 11. Dynatup impact strength (standard notch) vs dissipative energy density (u_d) for 6.35 mm thick specimens of varying rubber phase composition.

geometrical factor given by

$$Y = 1.93 - 3.07(a/W) + 14.53(a/W)^2 - 25.11(a/W)^3 + 25.80(a/W)^4. \quad (9)$$

Plain-strain conditions are expected when $a/W \leq 0.6$. According to Kudva et at [22], the failure stress given by Eq. (7) is smaller than that from Eq. (8) for short ligament (long cracks) and vice versa for long ligaments (short cracks). This explains in a qualitative way the ductile-to-brittle transition with ligament length shown in Fig. 7. Here, we compare these models with the experimental data to estimate the parameters σ_y and K_{IC}.

The solid lines in Fig. 12 represent the best fit of Eq. (7) to all the data where ductile failure was exhibited. This model does a satisfactory job of describing the results. For Fig. 12e and f there are too few ductile failures to justify such an analysis. The values of σ_y obtained from this data fitting procedure are listed in Table 6; the σ_y parameters from this fit decrease with increasing amount of EPR-*g*-MA in the blend which corresponds to smaller particles, higher levels of grafting, and reduced crystallinity. The absolute values of σ_y, obtained by the fit, are quite large compared to those obtained from simple tensile tests; of course, the yield strength is expected to be larger at higher strain rates but there are no data available for direct comparison at the strain rates ($\sim 10^3\ s^{-1}$) of this type of test. High-speed tensile data by Dijkstra et al. [32] indicate a rapid increase in yield stress as the strain rate approaches the levels estimated for the current test; thus, the estimates in Table 6 may be plausible.

The dotted lines in Fig. 12 represent the best fit of Eqs. (8) and (9) to the brittle failure stresses (limited to conditions where plane-strain is expected). Table 6 lists the values of K_{IC} obtained by this fitting procedure. Since brittle fracture was not observed in Fig. 12 a–c, no values of K_{IC} were deduced for these compositions. The values of the K_{IC} parameter obtained in this way increase with increasing EPR-*g*-MA content in the blend. Adams reported a K_{IC} value of 3.0 MPa $m^{1/2}$ for Zytel 101 (nylon 6,6) tested in an impact mode (1 m/s) similar to the method reported here [33]. The values reported in Table 6 are in the same range.

5. Conclusions

Fracture behavior of toughened nylon 6 blends of varying rubber particle size was examined by Izod and SEN3PB type tests using injection molded specimens of two thickness with sharp notches and varying ligament lengths. Plots of specific fracture energy vs ligament length were linear when ductile failure occurred; values of the limiting specific fracture energy (u_o) and the dissipative energy density (u_d) were obtained and discussed.

When there is 50% or more of the reactive EPR-*g*-MA in the rubber phase ($\bar{d}_w = 0.24$ to 0.61 μm), super tough blends were obtained under all testing conditions; the specific fracture energy showed a linear relationship vs ligament length with very little scatter. The impact strength of these specimens was generally insensitive to which end of the bar that was tested. The same range of impact fracture energies was obtained with thick and thin specimens and by using either the Izod or Dynatup tests.

Blends that contained 37.5% or less of EPR-*g*-MA and where the rubber particle size was 0.75 μm or higher were more sensitive to sample dimensions, location along the bar, and test configuration. A dual mode of fracture was observed, depending on ligament length, for blends which had a ductile to brittle transition temperature near room temperature or higher; the specimens with short ligaments fractured in a ductile manner and gave high values of the specific fracture energy, while the specimens with long ligaments showed brittle fracture and gave lower values of energy. A dual mode of fracture was observed for both Izod and SEN3PB tests. The critical ligament length at which the ductile-to-brittle transition occurred increased with increasing amount of EPR-*g*-MA in the blend, i.e. with decreasing rubber particle size. The change from ductile failure at short ligament length to brittle failure at longer ligaments for these transitional materials was rationalized in terms of classical equations for ductile yielding and brittle crack propagation. Values of the yield stress and critical stress intensity factor were estimated from the data using these model equations.

The parameter u_d was found to be more sensitive to rubber particle size, sample thickness and location in the molded bar than u_o. A good correlation between the standard

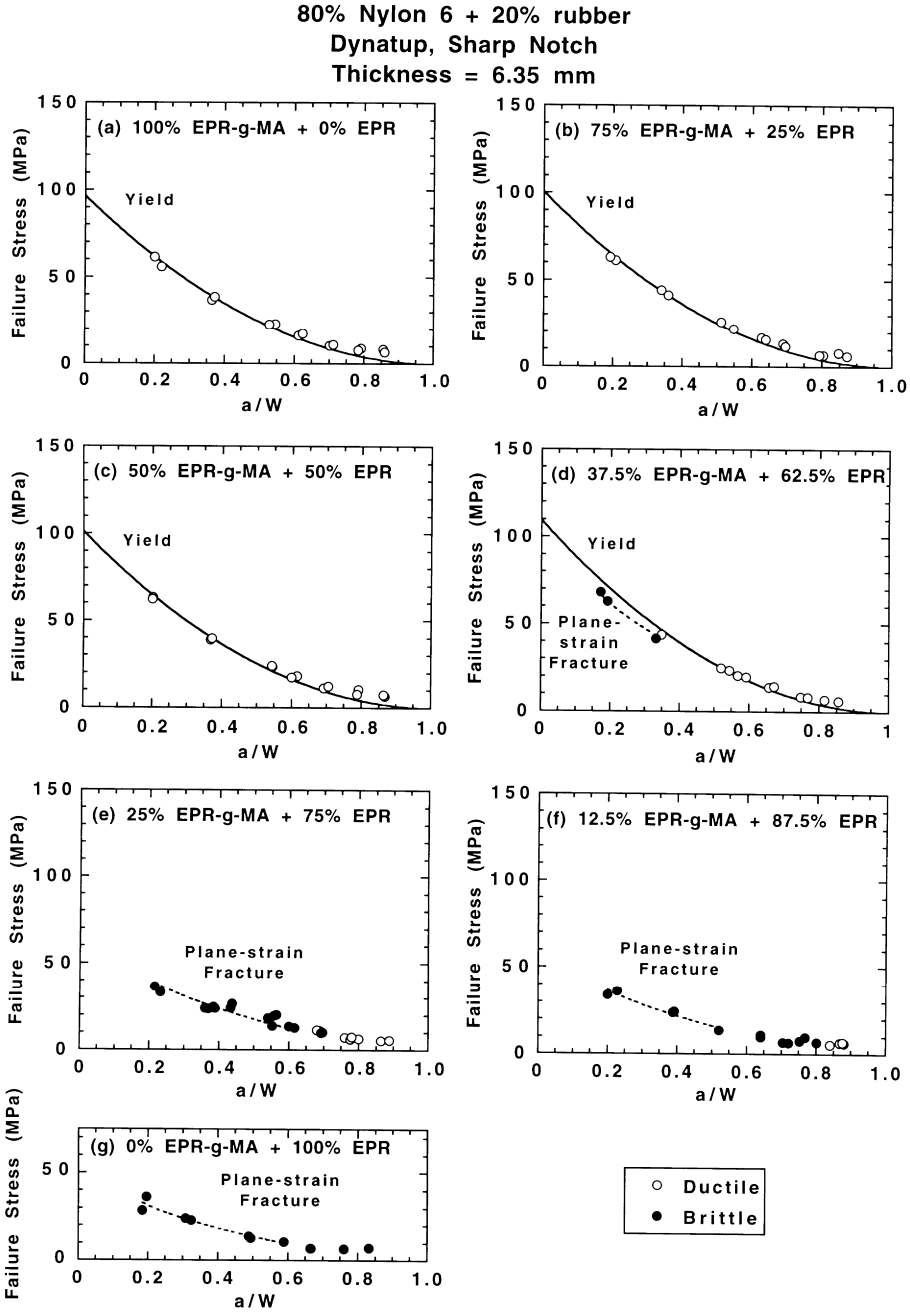

Fig. 12. Failure stress as a function of crack length (a/W) from Dynatup measurements on thick specimens with a sharp notch for blends of 80% nylon 6 and 20% maleated EPR mixture. (○) ductile break, (●) brittle break.

Dynatup impact strength and the parameter u_d was observed for the gate end specimens.

Acknowledgements

This research was supported by Bridgestone Corporation. The authors express their appreciation to AlliedSignal Inc. and Exxon Chemical Co. for their assistance with various materials used in this research. The authors wish to thank Yoshihiro Kayano and Ryan A. Kudva for many helpful suggestions and discussions.

References

[1] Wu S. Polym Engng Sci 1987;27:335.
[2] Wu S. J Appl Polym Sci 1988;35:549.

[3] Lawson DF, Hergenrother WL, Matlock MG. J Appl Polym Sci 1990;39:2331.
[4] Gilmore DW. Plastics Engng 1989;45:51.
[5] Hobbs SY, Bopp RC, Watkins VH. Polym Engng Sci 1983;23:380.
[6] Oshinski AJ, Keskkula H, Paul DR. J Appl Polym Sci 1996;61:623.
[7] Oshinski AJ, Keskkula H, Paul DR. Polymer 1996;37:4909.
[8] Oshinski AJ, Keskkula H, Paul DR. Polymer 1996;37:4919.
[9] Kayano Y, Keskkula H, Paul DR. Polymer 1997;38:1885.
[10] Kayano Y, Keskkula H, Paul DR. Polymer 1998;39:2835.
[11] Borggreve RJM, Gaymans RJ, Schuijer J, Housz JFI. Polymer 1987;28:1489.
[12] Borggreve RJM, Gaymans RJ. Polymer 1988;29:1441.
[13] Borggreve RJM, Gaymans RJ. Polymer 1989;30:63.
[14] Oshinski AJ, Keskkula H, Paul DR. Polymer 1996;37:4891.
[15] Chung I, Throckmorton E, Chunury D. Soc Plast Engng. ANTEC 1979;25:681.
[16] Broberg KB. Int J Fract 1994;21:83.
[17] Mai Y, Powell P. J Polym Sci Part B: Polym Phys 1991;29:785.
[18] Mai Y. Int J Mech Sci 1993;35:995.
[19] Mai Y. Polymer Commun 1989;30:330.
[20] Vu-Khanh T. Polymer 1988;29:1979.
[21] Wildes G, Keskkula H, Paul DR. Polymer 1999;40:7089.
[22] Kudva RA, Keskkula H, Paul DR. Polymer 2000;41:335.
[23] Flexman EA. International conference: toughening of plastics. London: The Plastics and Rubber Inst, 1978 (p. 14).
[24] Flexman EA. Polym Mater Sci Engng 1990;63:112.
[25] Flexman EA. Soc Plast Engng. ANTEC 1984;30:558.
[26] Vu-Khanh T. Theor Appl Fracture Mech 1994;21:83.
[27] Mamat A, Vu-Khanh T, Cigana P, Favis BD. J Polym Sci Part B: Polym Phys 1997;35:2583.
[28] Wu J, Mai Y. Polym Engng Sci 1996;36:2275.
[29] McCrum NG, Buckley CP, Bucknall CB. Principles of polymer engineering. Oxford University Press, Oxford, 1988, p. 194–200.
[30] Gross B, Srawley JE. Stress-intensity factors for single-edge-notch specimens in bending or combined bending and tension by boundary collocation of a stress function. Technical Note. D-2603, NASA, 1965. p. 8.
[31] Brown WF, Srawley JE. ASTM 410, 1996. p. 13.
[32] Dijkstra K, Wevers HH, Gaymans RJ. Polymer 1994;35:323.
[33] Adams GC. Soc Plast Engng ANTEC 1988;34:1517.